

Interpretations of Chaff Trajectories Near a Severe Thunderstorm

EDWARD A. JESSUP—*National Severe Storms Laboratory, Environmental Research Laboratories, NOAA, Norman, Okla.*

ABSTRACT—A severe right-moving thunderstorm formed 60 n.mi. southwest of Norman, Okla., on June 25, 1969, and moved slowly northeastward. Eleven bundles of chaff were released upwind at an altitude of 15,000 ft mean sea level (msl) and within 15 n.mi. of the thunderstorm. Nine of the bundles were observed by radar to enter the pre-

cipitation echo of the storm. Three of these appeared to move through the precipitation and emerge from the downwind side of the storm. Airflow near the thunderstorm, determined from these trajectories, indicated that lee eddies were formed within air being diverted around the storm.

1. INTRODUCTION

During recent years, interest has grown concerning the relationship between severe thunderstorms and environmental airflow. Before World War II, most meteorologists agreed with Humphreys (1940) that the velocity of the thunderstorm is nearly the velocity of the atmosphere in which the bulk of the cloud is located. Since that time, thunderstorm studies have become more sophisticated with the advent of radar, high-altitude aircraft, and rawinsonde equipment. As Fankhauser (1964) mentions, accumulated evidence shows that small, uniform, non-propagating storms frequently move with the winds at a particular level (usually near 700 mb), but propagating cumulonimbi of various sizes do not. Thunderstorms have been observed to merge (Stout and Hiser 1955), split (Fujita and Grandoso 1968), and move to the right and left of the mean flow (Newton and Katz 1958, Harrold 1966, Hammond 1967). This suggests that the interaction of thunderstorm circulation with environmental flow is reflected in storm motion.

Three possible views of the general relationship between strong thunderstorms and environmental flow are (1) the thunderstorm acts as a barrier to environmental flow, (2) air flows through the thunderstorm with little resistance, or (3) thunderstorms are neither rigid barriers to environmental flow nor does air flow through them freely.

One of the tasks of the Storm Morphology and Dynamics Project at the National Severe Storms Laboratory (NSSL) has been the collection of data to examine these viewpoints. One technique involves the tracking of chaff bundles released in the vicinity of large thunderstorms. Fankhauser (1968) discussed a chaff experiment performed near NSSL in which 13 bundles were released at 500 mb both upwind and downwind of a mature right-moving severe thunderstorm. His analysis indicated that most of the bundles tended to flow around the storm. A single bundle was observed, however, to merge with the precipi-

tation echo. These observations suggested to him that the mature thunderstorm acted as an effective barrier to middle tropospheric flow, although some of the ambient air simultaneously entered the thunderstorm.

In the spring of 1969, Weather Science Inc.,¹ under contract with the Environmental Science Services Administration (now National Oceanic and Atmosphere Administration), released chaff from aircraft near thunderstorms when requested by NSSL. Each chaff package was composed of approximately 400,000 aluminum-coated glass fibers. Each fiber was approximately 1 mil in diameter and cut to a length of 10.7 cm, the wavelength of the WSR-57 radar at NSSL. Manufacturer² specifications indicate a radar cross-section of 5,000 ft² per package. Tests performed by the U.S. Air Force for the manufacturer and independently at NSSL indicated that individual dry fibers have a terminal velocity near 0.50 kt when in still air. Additional tests at NSSL indicated that wet fibers have a terminal velocity near 0.80 kt. No data are available concerning fall rates when icing takes place. During our experiments, the chaff was released at a level below freezing to minimize icing influence.

Chaff positions were recorded by time-lapse photography of a WSR-57 plan-position indicator (PPI) scope. The time interval between each filmed scan was near 45 s. The NSSL radar display shows echo intensities contoured at reflectivity factor values (Z_e) of approximately 10^1 – 10^6 mm⁶·m⁻³ at 10^1 intervals. The NSSL radar system has been described by Wilk et al. (1968) and by Sirmans et al. (1970).

2. SYNOPTIC CONDITIONS

The atmosphere over Oklahoma early on June 25, 1969, was moderately conducive to severe thunderstorm formation. Surface and 500-mb depictions of an intense Low over

¹ Mention of a commercial company or product does not constitute an endorsement.

² Lundy Electronics and Systems, Inc., Glen Head, N. Y. 11545

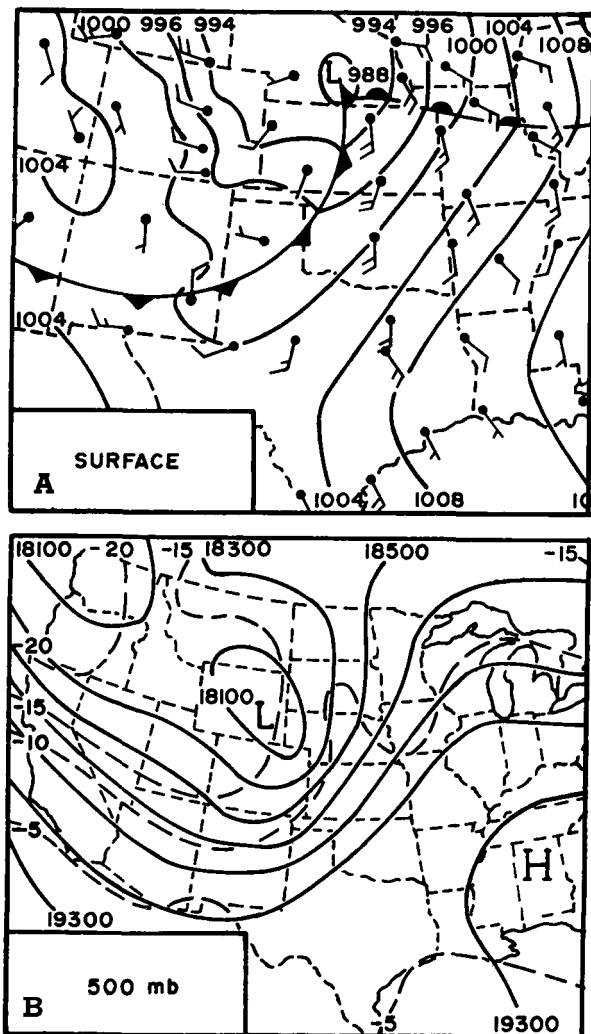


FIGURE 1.—The (A) surface and (B) 500-mb charts for 0600 CST on June 25, 1969 (prior to thunderstorm development).

the Great Plains are shown in figures 1A and 1B. Flow toward the Low was bringing warm, moist gulf air across Oklahoma at low levels and dry air aloft, thus providing two important ingredients for severe thunderstorm development. The weak cold front entering northwestern Oklahoma during the morning hours (fig. 1A) acted as a lifting mechanism over central Oklahoma later during the day. This, with a minor trough aloft and surface heating, caused thunderstorms to form during the afternoon.

At 1455 CST, a thunderstorm formed about 60 n.mi. southwest of Oklahoma City and moved to the northeast. Within an hour after its formation (1545 CST), the storm became mature and began to move to the right of the wind velocity at most levels as implied by the 1200 CST Tinker AFB wind sounding (not shown). At this time also, radar indicated that precipitation particles extended to 55,000 ft MSL. The most intense echoes associated with this storm moved at nearly 40 kt initially but slowed to less than 20 kt after the storm matured. As the storm vault passed near Choctaw, Okla., a suburb of Oklahoma City, a small tornado touched down and caused minor damage. Hail diameters measured up to 2 in., and winds in excess of 55 kt also occurred in nearby areas.

3. CHAFF TRAJECTORIES

Chaff Deployment

A single-engine Cessna with a cruising speed of 150 kt was used to place 11 bundles of chaff 5–10 n.mi. upstream from the thunderstorm. They were released between 1519 and 1553 CST at 15,000 ft MSL (average terrain near 1,200 ft MSL) at 5-n.mi. intervals, except the first two bundles which were separated by 3 n.mi. Nine were released in an L-shaped pattern along the northwestern and southwestern sides of the thunderstorm as indicated in figures 2A–2C. Two bundles, 10 and 11, were dropped west of bundle 9 but do not appear in figure 2.

The WSR-57 radar antenna tilt was fixed at 2° until all chaff was ejected. As bundle 11 was dropped, an automatic antenna tilt sequence from 1° to 4° at 1° increments was initiated. At first, each chaff bundle appeared as a point target on radar. After 30 min., however, several bundles had intensity contours of $Z_e \text{ max} = 10^3 \text{ mm}^6 \cdot \text{m}^{-3}$ and appear in figure 2.

Chafflike Echoes

Chaff was expected either to flow around the thunderstorm or to move into it and not be seen again. Surprisingly, however, of the nine chaff-bundle echoes that merged with the precipitation echo, three were apparently associated with chafflike echoes that later emerged from the downwind side of the storm. Two of these chafflike echoes were tracked within precipitation before they exited the storm. The following discussion explains why these three chafflike echoes are considered to be chaff. We will show that echoes known to be chaff and the chafflike echoes behaved similarly and not as precipitation echoes typically behave.

It seems reasonable that chaff may be tracked within precipitation from contoured PPI displays since chaff tends to enhance precipitation reflectivity. Sufficient enhancement will produce a region of greater reflectivity within precipitation that can be followed on radar. The horizontal motion of the chaff and the chafflike echoes in this storm is revealed by the WSR-57 PPI time-lapse film. Chaff bundles 1 and 2 did not enter the precipitation echo, thus allowing chafflike echoes to be compared with echoes known to be chaff. The two chafflike echoes that traveled within the precipitation echo (believed to be numbers 3 and 9) emerged from it and then moved away at a velocity similar to chaff.

Figure 2 helps to illustrate the movement and appearance of chaff and chafflike echoes. Bundles 1 and 2 in figures 2A–2M were followed continuously and can be seen to remain outside the precipitation echo. Both chaff (labeled 2) and chafflike echoes (labeled 3 and 9) in figures 2F–2M had a maximum reflectivity value of $Z_e = 10^3 \text{ mm}^6 \cdot \text{m}^{-3}$ as indicated by a small circular area. The chafflike echoes were visible within the precipitation echo and were followed along a smooth and continuous path. The echo labeled number 3 appears below bundle 2 at an indicated separation of 7 n.mi. in figure 2F, only 2 n.mi.

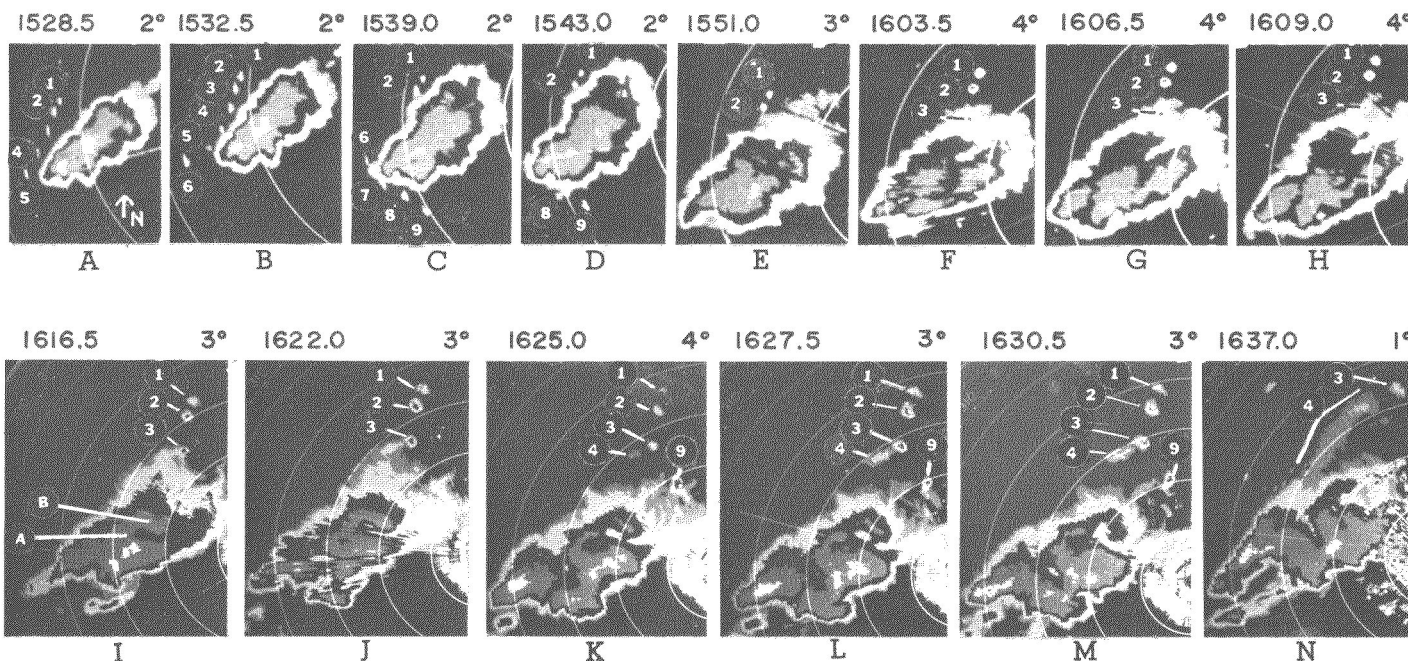


FIGURE 2.—WSR-57 PPI displays of chaff and precipitation at NSSL on June 25, 1969. All times are indicated to the nearest half minute (CST) at the top-left portion of each photo. Radar antenna elevation is presented at the top-right. Chaff echoes are numbered. The lettered arrows (after Lemon 1970) are A, the low-reflectivity intrusion of the eddy vortex, and B, the high-reflectivity crescent of the vortex.

greater than the initial separation of bundles 2 and 3. Figures 2F–2M show that they had a similar appearance on radar, moved similarly, and retained their relative separation as bundle 3 emerged from precipitation. Number 9 behaved likewise as indicated by figures 2K–2M.

One other chafflike echo (labeled 4) appeared on radar. It became evident at the downwind edge of the precipitation echo. Although figure 2N shows that it was plume shaped and thus different from other chaff echoes, it traveled in a manner similar to numbers 1, 2, 3, and 9.

All chaff and chafflike echoes slowly decreased in intensity and altitude but remained intact during the hour after chafflike echoes emerged from the storm. Figure 3 is a graph of the radar heights at which chaff and chafflike echoes returned maximum reflectivity. Curves labeled 1 and 2 pertain to echoes known to be chaff. Those numbered 3, 4, and 9 represent the chafflike echoes.

Both chaff and chafflike echoes had similar fall speeds that were significantly less than the terminal speed of precipitation with similar reflectivities in still air. Fall rates of chaff and chafflike echoes were determined from figure 3. An estimate of the rainfall rate at similar reflectivities (average maximum reflectivity between 10^2 and $10^3 \text{ mm}^6 \cdot \text{m}^{-3}$) was determined from the relationship

$$Z_e = 200r^{1.6}$$

to be about 0.06 in./hr, where Z_e is the observed reflectivity and r is the rainfall rate. The median raindrop diameter corresponding to this rainfall rate was determined to be 0.06 in. from the drop-size spectra data collected by Mueller and Sims (1966). They obtained this spectra using photographs collected from a camera sam-

pling raindrops at several sites around the world and under various rainfall regimes. The values cited here are the results obtained at Miami, Fla., during thunderstorm situations. A 0.06-in. diameter droplet has a terminal velocity of near 10.8 kt according to a study conducted by Gunn and Kinzer (1949). A comparison between the observed fall rates of the chaff and the chafflike echoes (0.36–1.88 kt) and those expected for precipitation (10.8 kt) indicated that precipitation fall rates were an order of magnitude greater.

Of course, both estimates are relative to still air. But to have assumed that the chafflike echoes were precipitation would have implied a large area of uniform upward air motion on the downwind side of the storm. Such a feature would have caused these echoes to intensify and increase in vertical extent. These echoes, however, behaved in the opposite sense. In light of the evidence discussed previously, we believe that the chafflike echoes were indeed chaff.

Horizontal Chaff Trajectories

Chaff trajectories relative to the storm are superimposed on the approximate envelope of the precipitation echoes during the period from 1519 to 1645 CST in figure 4. The hatched shading is the envelope of precipitation echoes with reflectivities $Z_e \geq 10^4 \text{ mm}^6 \cdot \text{m}^{-3}$. As noted before, bundles 1 and 2 were tracked continuously and remained outside the precipitation echo thus eliminating any doubt concerning their trajectories. Of the remaining 9 bundles that disappeared into the storm, three were later tracked again (Nos. 3, 4, 9). Time-lapse film, velocity computation, and extrapolation of chaff trajectories suggest that the three chaff bundles that emerged from the storm cor-

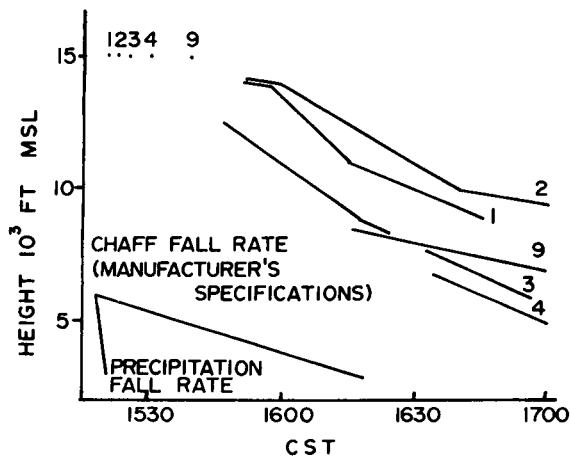


FIGURE 3.—Chaff and precipitation fall rates. Numbered lines correspond to chaff bundles 1, 2, 3, 4, and 9. The fall rate of precipitation with reflectivity similar to that of chaff is presented at the lower left.

respond to the like-numbered bundles on the upwind side of the storm as shown in figure 4.

Filmed PPI displays suggest that the chaff plume (No. 4) was possibly composed of two bundles. A reflectivity-volume product was formed for the plume and echo 2 by multiplying the reflectivity of each echo times the volume it occupied. The reflectivity of number 2 was considered as representative of what was expected from just one bundle, since it remained outside the storm and intact. The volume was defined as the sum of the products of echo areal display at various antenna tilt angles times the average vertical depth equivalent to 1° of arc, the incremental angles between successive PPI photographs. The ratio of the reflectivity-volume products between the plume and chaff bundle number 2 was about two, implying that the plume contained two bundles, possibly 4 and 5 since they were released nearest bundle 3. The plume, however, is designated as number 4 for convenience. Numbers 3 and 9 were similarly compared to number 2, and it appears that they were composed of only their original chaff.

The remaining chaff, bundles 6, 7, 8, 10, and 11, apparently entered the storm and were not seen again. They entered where strong updrafts and downdrafts probably were occurring near each other. It is reasonable to assume that these bundles either traveled upward and left the storm aloft or were forced down by heavy precipitation and/or downdrafts.

4. RELATIVE AIRFLOW

Discussion in this section indicates that this storm was well ventilated at midlevels except in a relatively small region near the hook echo where blocking was apparent. In the lee of the blocking vortex, there is some evidence of eddy generation.

Wind speeds relative to the precipitation echo appearing in figure 4 were derived from 5-min changes in chaff positions from 1525 to 1555 cst. Isotachs were analyzed

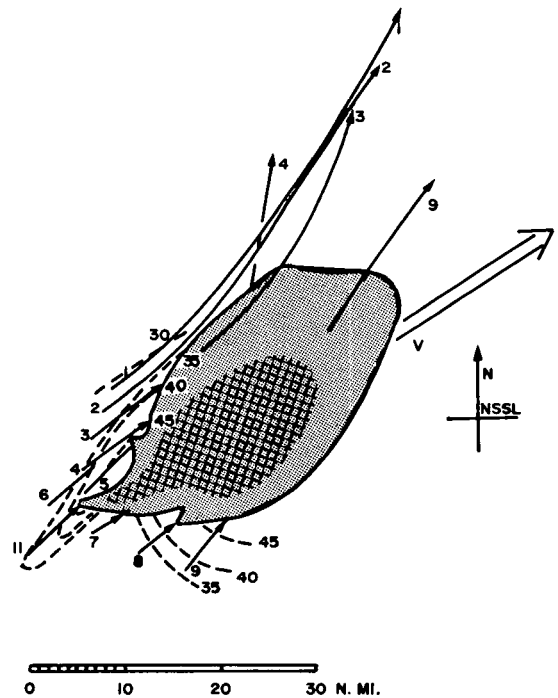


FIGURE 4.—Chaff trajectories (solid) and isotachs (dashed) relative to composite precipitation echo. Thunderstorm motion is indicated by the double arrow.

along the upwind side of the storm where chaff was dropped at 15,000 ft msl. An isotach analysis downstream from the thunderstorm reveals that similar speed values were present there, but the analysis is not found in figure 4 because chaff at that side of the storm was present at various levels.

Thunderstorm ventilation and resistance to flow are both indicated by the flow pattern appearing in figure 4. Nearly parallel flow was present entering and emerging from the right and left flanks of the storm where low-reflectivity precipitation echoes were located. This observation, along with the high speed of the relative wind in the same regions, suggests that these portions of the storm were well ventilated. Resistance to airflow was found along the upwind side of the thunderstorm near the hook-shaped echo. The pattern resembles that found within fluid flow along the upflow side of a solid circular cylinder; diffuence was indicated by the separation of bundles 5 and 6 from bundles 7 and 8 on either side of the hook where a speed minimum appears in figure 4. The flow pattern is also consistent with the general observation that ambient flow is deflected around vortices; intense hook-shaped echoes have been related to cyclonic rotation (Fujita 1958) and to vertical motion (Browning and Donaldson 1963), which, in turn, has been related to blocking of environmental airflow (Hitschfeld 1960).

Similar flow patterns near thunderstorms have been suggested by others. Thunderstorm ventilation and resistance to flow was noted by Donaldson et al. (1969) and by Kraus (1970) in their investigation of the flow within an isolated right-moving severe thunderstorm near Marblehead, Mass. Wind components along the Doppler radar radial within that storm indicated that it was

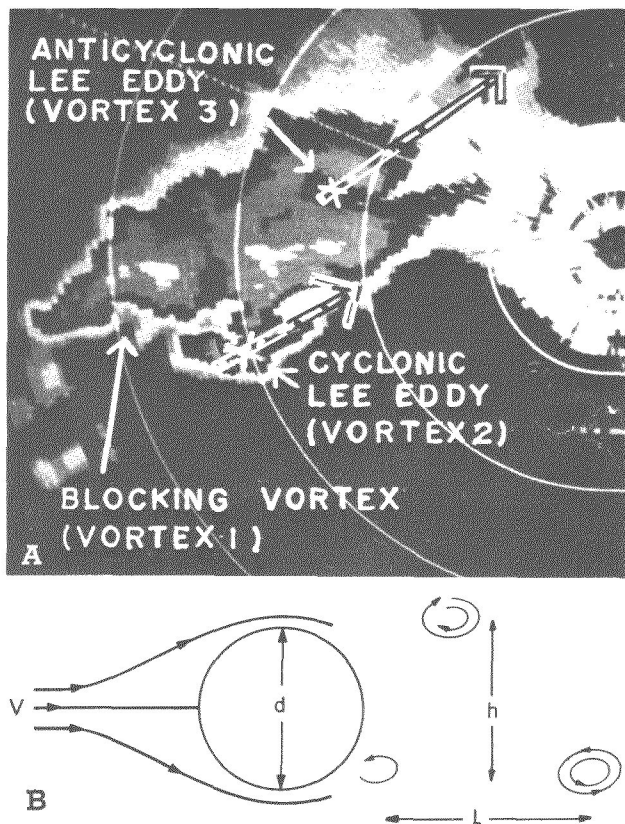


FIGURE 5.—(A) radar echo patterns at 1620 CST on June 25, 1969, at an antenna elevation of 4° . The patterns resemble a Kármán vortex train if vortices 2 and 3 are considered as lee eddies downstream from vortex 1. Arrows represent the direction of relative motion of the lee eddies from 1616 to 1655 CST. Dots along the arrows indicate approximate 10-min positions of vortex centers. Xs represent the centers at photograph time. (B) schematic diagram representing a vortex trail produced by an incompressible fluid moving past a solid right-circular cylinder under laboratory conditions.

ventilated both along its upwind and downwind sides. Blocking by the updraft portion of the storm was inferred from regions of speed minima believed to be associated with wake phenomena.

The flow along some fringes of the June 25 storm was apparently smooth both inside and outside the precipitation echo. Remarks made by the aircraft pilot after chaff was ejected indicated that no turbulence was experienced, and radar indicated that chaff bundles 1, 2, 3, and 9 dispersed only slowly with time. This was true although vertical velocity estimates indicated that air near bundles 3 and 9 traveled downward after entering the precipitation.

A more turbulent record, however, was indicated by the shape of number 4, which apparently traveled near echo reflectivities $Z_e = 10^4 \text{ mm}^6 \cdot \text{m}^{-3}$. After this bundle emerged from precipitation, it was plume shaped and trailed downward toward the storm from near 10,000 ft (the same altitude as number 3) to about 5,000 ft MSL for a distance of 20 n.mi. Apparently, this chaff was subjected to downward motion, vertical shear, turbulence, precipitation scavenging, or some combination of these.

Lemon (1970) studied another aspect of this storm during a time period that overlaps this study. He observed

that a convergent anticyclonic eddy vortex (fig. 5A) apparently developed and then emerged from the downwind side of the storm in the region between bundle number 9 and numbers 3 and 4. Number 9 had a tail (figs. 2K, 2M) that was oriented nearly perpendicular to its direction of motion. It seems plausible that the tail was drawn away from the main body of chaff by the anticyclonic vortex (visible in figs. 2I–2M) as its circulation spread to include air near number 9. Although the air near number 3 apparently moved downward after entering precipitation, it did not appear to be drawn into the anticyclonic circulation. Instead it moved as if it were embedded in parallel flow. The same may have been true of air near number 4 although it apparently moved nearer the developing eddy. Its motion is less well explained because of the uncertain causes of its plume shape.

Briefly stated, midlevel relative streamlines constructed from chaff trajectories indicate that this storm was well ventilated except in a relatively small region near the hook echo where blocking was apparent. In the lee of the blocking vortex, there is some evidence of eddy generation.

Much of the following discussion concerns various aspects of the anticyclonic eddy, and it should be acknowledged that Lemon's (1970) paper is the primary source of that information.³ An attempt was made to construct the horizontal flow pattern at midlevels (near 12,000 ft MSL) in the vicinity of the thunderstorm both from chaff and from contoured PPI radar presentations. Time-lapse movies of radar PPI presentations indicated three regions of rotation. They are labeled as vortices 1–3 in figure 5A. Although horizontal airflow implied from radar presentations is difficult to derive and can be misleading, time-lapse movies of this storm indicated that the horizontal precipitation echo motions were consistent with chaff motions. This, together with Lemon's study, indicates that flow patterns implied from PPI presentations represent the horizontal airflow fairly well. Figure 5A condenses the results of the time-lapse film study of this storm. The persistent vortex patterns show a close resemblance to those of lee vortex generation found in laboratory experiments studying fluid flow past a solid right cylinder. In such a comparison, vortices 1, 2 (cyclonic), and 3 (anticyclonic) replace the cylinder and its lee vortices, respectively.

Experiments (Prandtl and Tietjens 1957) have shown that eddies are generated regularly from a rotating cylinder when the ratio of the cylinder rim speed, u , to the ambient fluid speed, v , varies from 9 (no rotation) to at least $1/2$ and when the Reynolds number of the fluid, $Re = vdp/\mu$, varies from 10^3 to 10^5 , where d is the diameter of the cylinder, ρ is the density of the fluid, and μ is the fluid coefficient of viscosity. Vortices forming on either side of the cylinder, as pictured in figure 5B, have opposite directions of rotation and form a geometric pattern of alternating cyclonic and anticyclonic vortices to the lee

³ Lemon offered three possible explanations for the anticyclonic eddy. He considered that it may have been related to a nonsteady rotation of the updraft and was, therefore, a "starting vortex," it could have been created by a systematic flow in which the conservation of three-dimensional vorticity was prominent, or it may have been of the Kármán type shed from vortex 2 in figure 5B.

of the obstacle. They entrain environment fluid only slowly, move at a speed slower than the ambient flow, and eventually dissipate by internal friction. Von Kármán⁴ proved that vortex trails have a geometric pattern that is "generally unstable" resulting in deviations from the pattern seen in figure 5B. Neutral stability occurs at a value of $h/L=0.28$ (for nonrotating cylinder) where h and L are the cross-distance and wavelength as indicated in the figure. The value of this ratio is difficult to measure accurately when a single vortex pair is present because the tendency for instability does not allow one to measure h and L with confidence over a sufficient length of time. No estimate of the value of this ratio for the June 25th storm appears here for this reason.

The similarity between the flow pattern of these laboratory experiments and that of figure 5A is striking. Storm vortices 2 and 3 became well defined at about 1615 CST to the lee and on either side of vortex 1. They rotated in opposite senses and traveled downstream from vortex one in a direction very nearly that of the mean wind ($250^\circ/50$ kt as determined at midlevels from the noon Tinker AFB sounding) but at a slower speed. Both eddies traveled about 20 kt relative to vortex 1 as the anticyclonic eddy became visible at 1615 CST, but speed differences arose as the anticyclonic eddy accelerated and the cyclonic eddy decelerated. Their relative speeds at 1655 CST were near 35 and 10 kt, respectively, as precipitation associated with the anticyclonic eddy disappeared.

Although the results of the time-lapse film study are consistent with lee vortex generation, it cannot be resolved whether or not such a phenomenon actually contributed to the circulation of the thunderstorm under study. Evidence both pro and con may be cited. Evidence against vortex generation is the fact that the Reynolds number for the situation on this date was found to be considerably greater (near 10^9) than the critical value determined experimentally (always true for the atmosphere). Laboratory results, however, were based on fluid flow around a solid obstacle by an incompressible fluid. The Reynolds number values no doubt would be different for compressible fluid flow around a vortex composed of the fluid itself, especially in the presence of mixing between the vortex and its surroundings. To the author's knowledge, comparable experiments have not been performed, and no one can reliably say what values of Reynolds number are appropriate.

There is evidence that suggests that Kármán vortex trails do occur in the atmosphere on this scale. Friday and Wilkins (1967) described vortex trail phenomena in the lee of the Guadalupe and Cape Verde Island groups. Such trails were observed in the lee of 15 different islands from the Gemini photographs alone. One example appears in figure 6. In this Gemini 5 photograph, an eddy pattern resembling a Kármán vortex trail is present in the lee of Guadalupe Island off the southwestern California coast (max. height 4,500 ft MSL) at 1414 CST on Aug. 21, 1965. Friday and Wilkins found two apparent prerequisites for

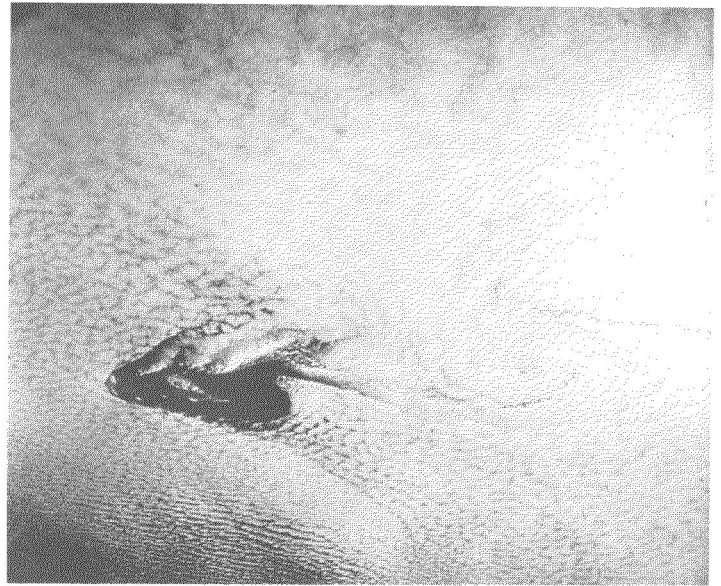


FIGURE 6.—Vortexes to the lee of Guadalupe Island as photographed at 1414 CST on Aug. 21, 1965.

vortex trail formation: steep slopes or bluff objects and a high degree of vertical stability (an inversion). They believed that the inversion would cause a relatively larger portion of the air to flow around the island instead of over it. These two prerequisites are apparently met near a mature thunderstorm. Vertical updrafts tend to block environmental flow much as steep mountain slopes and the stratospheric inversion tends to cause environmental air to flow around the updraft rather than over it. Zimmerman's (1969) studies of similar vortex trails also suggest that much of the Kármán theory may be successfully applied to atmospheric mesoscale eddy patterns. Other studies have been made by Hubert and Krueger (1962) and Chopra and Hubert (1964, 1965).

A study by Fujita and Grandoso (1968) indicates that eddies were observed to the lee of convective thunderstorm towers on Apr. 3, 1964. The contoured radar display of storms on this date led them to propose that wake vortexes developing to the lee of a mature thunderstorm caused it to split into cyclonically and anticyclonically rotating storms that moved to the right and left of the previous trajectory, respectively.

On June 25th, the strongest evidence supporting the vortex generation concept was the behavior of chaff near the storm. The occurrence of a speed minimum where midlevel air was being deflected just upstream from vortex 1 is significant since this implies that the vortex is capable of blocking environmental flow. The presence of the tail of number 9 on the downwind side of the eddy is consistent with precipitation echo analyses implying that air was being drawn into the eddy. Downward motion was indicated near the anticyclonic vortex by bundle 3 traveling upwind from it, in agreement with Lemon's (1970) analyses.

The streamline pattern constructed from chaff trajectories at the fringe of the storm is in good general agree-

⁴ Prandtl and Tietjens (1957), p. 131

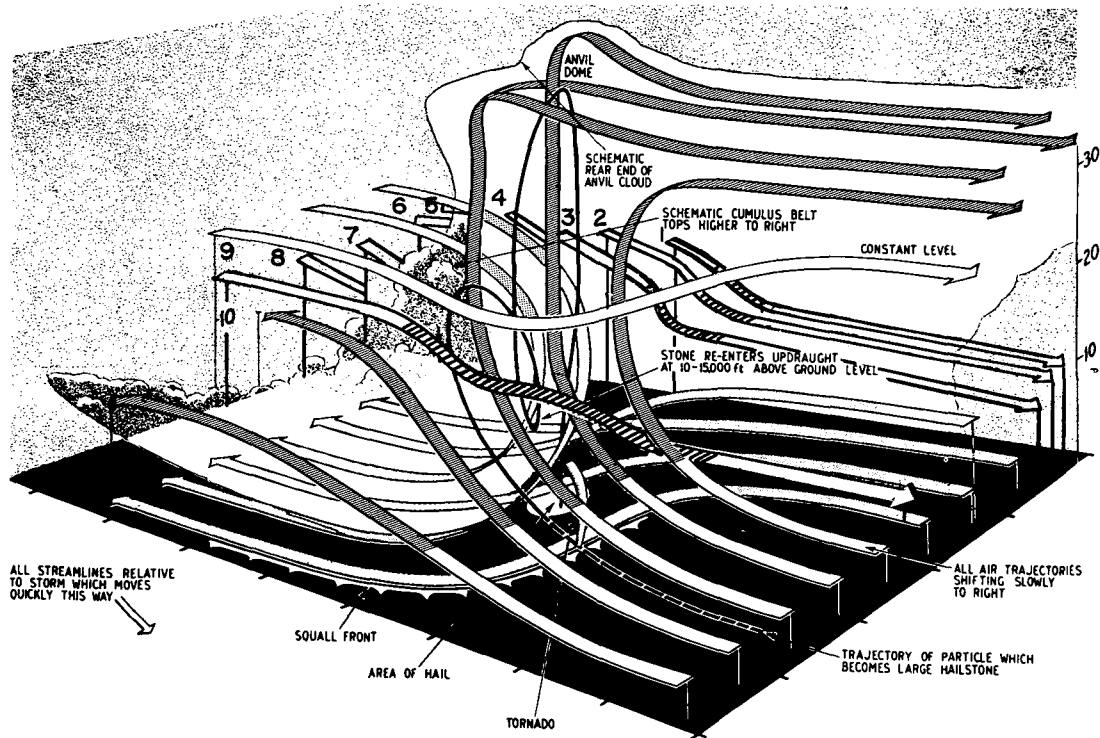


FIGURE 7.—Three-dimensional model of relative airflow within a mature severe thunderstorm (after Browning and Ludlam 1962). Numbered streamlines were constructed from chaff trajectories with darkened portions representing flow within precipitation.

ment with the right-moving mature severe thunderstorm models of Browning and Ludlam (1962), Browning (1964), and Fankhauser (1971), suggesting that environmental flow patterns of this storm differed little from these recent models. Storm streamlines are superimposed over schematic representations of these two models in figures 7 and 8. Fankhauser's model is especially appropriate since rotation (possibly corresponding to vortex 1) is incorporated. In both models, low-level air along the right forward quadrant relative to the storm's motion is the main source of updraft air while midlevel air entering precipitation on the upwind side of the storm is the primary contributor to the downdraft.

Only a small change of these model streamlines is needed to accommodate a flow pattern leading to the development of lee eddies. Let us consider a thunderstorm with a flow similar to that in figure 7. At this stage of maturity no rotation is evident, but a mechanism that can lead to the development of a vortex is present. Midlevel air entering the upwind side of the storm becomes negatively buoyant as a result of evaporative cooling and rushes downward, creating a dome of cool air that tends to spread outward in all directions. The pressure gradient associated with this meso-High extends ahead of the rain-cooled air into the low-level environmental air, causing it to decelerate and approach a calm that is often observed at low levels near the edge of the meso-High. This results in cyclonic shear in the environmental air near the interface where lifting takes place. Lifting releases instability, and convection results. Low-level air converges to replace the lifted air and may enhance the initial cyclonic vorticity. Suf-

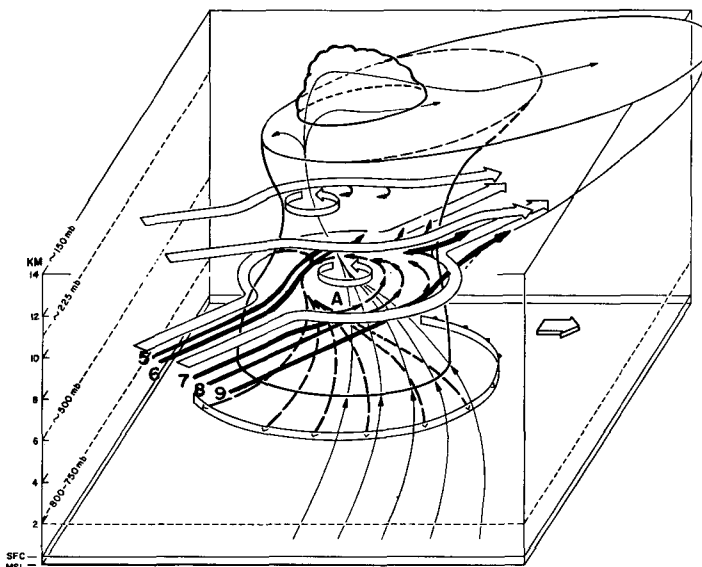


FIGURE 8.—Three-dimensional interpretation (after Fankhauser 1971) of the interacting external and internal airflow associated with an individual persistent Great Plains cumulonimbus. The thin, solid streamlines represent moist air originating in the subcloud layer (surface to ≈ 750 mb). The heavy dashed streamlines trace the entry and descent of potentially cold and dry middle-level (700-400 mb) air that feeds the downrushing and diverging downdraft. The surface boundary between the inflow and downdraft is shown as a barbed band. The internal circular bands signify net rotation of the updraft. The shape and orientation of the dividing external bands represent typical vertical shear and character of ambient relative horizontal airflow at middle (≈ 500 mb) and upper (≈ 225 mb) levels. The broad flat arrow on the right represents direction of travel. Solid arrows indicate flow patterns derived from time-lapse movies of chaff.

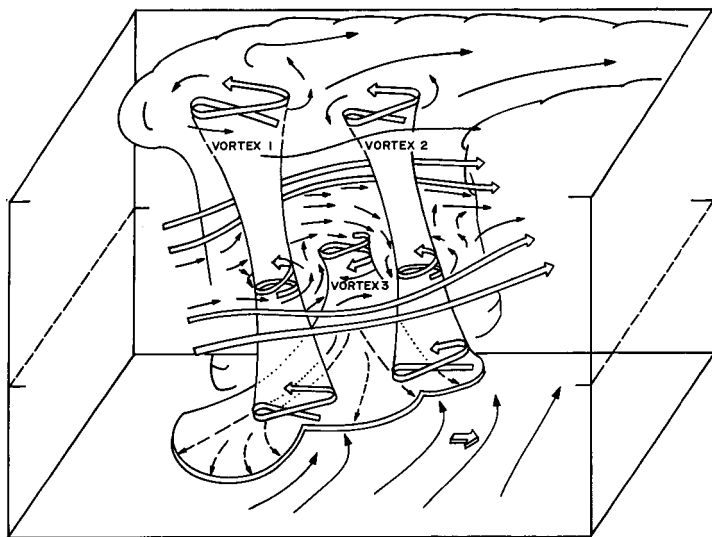


FIGURE 9.—Schematic representing relative flow that is consistent with lee vortex formation. Horizontal flow is represented by solid, thin arrows, spiraling vertical motion is indicated by double, corkscrew arrows, midlevel environmental air is represented by double, gently curving arrows, and rain-cooled downrushing air is represented by the dashed arrows that terminate at the mesocold front. Storm motion is indicated by the short, broad arrow near the bottom of the figure.

cient convergence may produce a cyclonic vortex (corresponding to vortex 1). We may then have a thunderstorm flow pattern similar to that seen in Fankhauser's model.

Only one step more is required to obtain the Kármán vortex train. Figure 9 is a schematic representing a possible airflow pattern that seems consistent with this next step. It is admittedly speculative and will be difficult for many readers to accept at first reading. We believe, however, that it is a reasonable explanation that is consistent with the interpretations and observations of the June 25th storm. Consider that midlevel environmental air diverted around the rotating thunderstorm updraft (vortex 1) may have led to the generation of lee eddies at midlevels in much the same way that flow around solid objects generates lee eddies. The column of rotating air associated with the cyclonic lee eddy implies a relative pressure deficit near its vortex center, since a continual acceleration (pressure gradient force) is required to deflect air movement from straight line flow. This circumstance induces some degree of upward motion in the column from below and could enhance eddy development at low levels especially if it is above a region of lifting at low levels. This would provide a favored location for cyclonic eddy development from near the surface to midlevels. Storm analyses on June 25th indicated that such a situation was consistent with observation; that is, a surface meso-High interface extended downstream from the blocking vortex (vortex 1) beneath the region where cyclonic lee eddy generation could be expected. Thus, it seems plausible that vortex 2 may have been generated in this way.

Vortex 3, the anticyclonic vortex, may have developed as follows: midlevel air entering precipitation in the lee

of the blocking vortex would become rain cooled and move downward, causing the air at midlevels to converge and replace the sinking air. In the region of anticyclonic vorticity (generated lee eddy), converging air would enhance this motion so that an anticyclonic downdraft could result (vortex 3). The anticyclonic downdraft described previously in this paper was located near the region where anticyclonic lee eddy generation would be expected. Therefore, it seems reasonable that vortex 3 could have developed in this way.

5. SUMMARY AND CONCLUDING REMARKS

On June 25, 1969, chaff was released upstream from an isolated severe thunderstorm within which an eddy pattern resembling a Kármán vortex train was developing. Relative chaff trajectories provided much of the supporting evidence. A speed minimum was discovered upstream from a hook echo in a region of diffluence indicating resistance to environmental flow. Rough estimates of vertical motion indicated that the anticyclonic lee eddy at midlevels was composed of downward moving air, thus supplementing Lemon's analysis, and some chaff was apparently drawn toward the anticyclonic eddy, indicating convergence. It was particularly interesting to discover that such an event seems reasonable with only a slight modification of current severe thunderstorm model flow patterns.

Radar patterns consistent with a development of this kind may not be uncommon. Research of radar film with contoured PPI displays indicates that similar patterns have appeared on a number of occasions during the last several years. When radar echo contouring becomes established across the United States, it may be found that such patterns are relatively frequent along thunderstorm lines in which individual storms tend to move parallel to the line.

Future experiments should supply additional information in other regions of severe thunderstorms such as the flow around or through the anvil and the subcloud inflow layer. Chaff represents an inexpensive tracer for determining horizontal trajectories both near and, occasionally, in thunderstorms. In addition, qualitative information on dispersion rates is obtainable. Finally, the combination of information obtained from chaff trajectories with data from other sources (Doppler radar, surface, aircraft, and sounding data) should provide a more complete picture of severe thunderstorm morphology.

ACKNOWLEDGMENTS

The author wishes to express thanks to Stanley L. Barnes, C. L. Jordan, and Edwin Kessler for their constructive criticisms and encouragement; to Ronald L. Shelton, whose patience and desire for perfection made good quality time-lapse movies possible; to Joseph Golden, who provided the satellite photograph; and to Charles Clark who prepared the figures.

A special debt of gratitude is owed to Neil B. Ward who was always ready to share his knowledge and understanding of the atmosphere.

REFERENCES

- Browning, Keith A., "Airflow and Precipitation Trajectories Within Severe Local Storms Which Travel to the Right of the Winds," *Journal of the Atmospheric Sciences*, Vol. 21, No. 6, Nov. 1964, pp. 634-639.
- Browning, Keith A., and Donaldson, R. J., Jr., "Airflow and Structure of a Tornadoic Storm," *Journal of the Atmospheric Sciences*, Vol. 20, No. 6, Nov. 1963, pp. 533-545.
- Browning, Keith A., and Ludlam, F. H., "Airflow in Convective Storms," *Quarterly Journal of the Royal Meteorological Society*, Vol. 88, No. 376, London, England, Apr. 1962, pp. 117-135.
- Chopra, K. P., and Hubert, Lester F., "Kármán Vortex-Streets in the Earth's Atmosphere," *Nature*, Vol. 203, No. 4952, MacMillan Journals, Ltd., London, England, Sept. 26, 1964, pp. 1341-1343.
- Chopra, K. P., and Hubert, Lester F., "Mesoscale Eddies in Wake of Islands," *Journal of the Atmospheric Sciences*, Vol. 22, No. 6, Nov. 1965, pp. 652-657.
- Donaldson, R. J., Jr., Armstrong, G. M., Chmela, A. C., and Kraus, M. J., "Doppler Radar Investigation of Air Flow and Shear Within Severe Thunderstorms," *Preprints of papers presented at the Sixth Conference on Severe Local Storms, Chicago, Illinois, April 8-10, 1969*, American Meteorological Society, Boston, Mass., 1969, pp. 146-154.
- Fankhauser, James E., "On the Motion and Predictability of Convective Systems as Related to the Upper Winds in a Case of Small Turning of Wind With Height," *National Severe Storms Project Report No. 21*, U.S. Department of Commerce, Weather Bureau, Washington, D.C., Jan. 1964, 36 pp.
- Fankhauser, James C., "Thunderstorm-Environment Interactions Revealed by Chaff Trajectories in the Mid-Troposphere," *ESSA Technical Memorandum ERLTM-NSSL 39*, U.S. Department of Commerce, National Severe Storms Laboratory, Norman, Okla., June 1968, 14 pp.
- Fankhauser, James C., "Thunderstorm-Environment Interactions Determined From Aircraft and Radar Observations," *Monthly Weather Review*, Vol. 99, No. 3, Mar. 1971, pp. 171-192.
- Friday, Elbert W., Jr., and Wilkins, Eugene M., "Experimental Investigations of Atmospheric Wake Vortex Trails. Part 1: Apparatus and Preliminary Results," *Research Institute Final Report ARL-1576-2*, ESSA Satellite Laboratory Research Grant E-41-67(G), University of Oklahoma, Norman, 1967, 58 pp.
- Fujita, Tetsuya, "Mesoanalysis of the Illinois Tornadoes of 9 April 1953," *Journal of Meteorology*, Vol. 15, No. 3, June 1958, pp. 288-296.
- Fujita, Tetsuya, and Grandoso, Hector, "Split of a Thunderstorm Into Anticyclonic and Cyclonic Storms and Their Motion as Determined From Numerical Model Experiments," *Journal of the Atmospheric Sciences*, Vol. 25, No. 3, May 1968, pp. 416-439.
- Gunn, Ross, and Kinzer, Gilbert D., "The Terminal Velocity of Fall for Water Droplets in Stagnant Air," *Journal of Meteorology*, Vol. 6, No. 4, Aug. 1949, pp. 243-248.
- Hammond, George R., "Study of a Left Moving Thunderstorm of 23 April 1964," *ESSA Technical Memorandum IERTM-NSSL 31*, U.S. Department of Commerce, National Severe Storms Laboratory, Norman, Okla., Apr. 1967, 75 pp.
- Harrold, T. W., "A Note on the Development and Movement of Storms Over Oklahoma on May 27, 1965" *ESSA Technical Memorandum IERTM-NSSL 29*, U.S. Department of Commerce, National Severe Storms Laboratory, Norman, Okla., Nov. 1966, pp. 1-8.
- Hitschfeld, Walter, "The Motion and Erosion of Convective Storms in Severe Vertical Wind Shear," *Journal of Meteorology*, Vol. 17, No. 3, June 1960, pp. 270-282.
- Hubert, Lester F., and Krueger, A. F., "Satellite Pictures of Mesoscale Eddies," *Monthly Weather Review*, Vol. 90, No. 11, Nov. 1962, pp. 457-463.
- Humphreys, William Jackson, *Physics of the Air*, 3d Edition, McGraw-Hill Book Co., Inc. New York, N.Y., 1940, 676 pp.
- Kraus, Michael J., "Doppler Radar Investigation of Flow Patterns Within Severe Thunderstorms," *Preprints of papers presented at the 14th Radar Meteorology Conference, Tucson, Arizona, November 17-20, 1970*, American Meteorological Society, Boston, Mass., 1970, pp. 127-132.
- Lemon, Leslie R., "Formation and Emergence of an Anticyclonic Eddy With a Severe Thunderstorm as Revealed by Radar and Surface Data," *Preprints of papers presented at the 14th Radar Meteorology Conference, Tucson, Arizona, November 17-20, 1970*, American Meteorological Society, Boston, Mass., 1970, pp. 323-328.
- Mueller, E. A., and Sims, A. L., "Investigation of the Quantitative Determination of Point and Areal Precipitation by Radar Echo Measurements," *Technical Report ECOM-0032-F*, Atmospheric Sciences Laboratory, U.S. Army Electronics Command, Ft. Monmouth, N.J., Dec. 1966, 88 pp.
- Newton, Chester W., and Katz, Sey, "Movement of Large Convective Rainstorms in Relation to Winds Aloft," *Bulletin of the American Meteorological Society*, vol. 39, No. 3, Mar. 1958, pp. 129-136.
- Prandtl, Ludwig, and Tietjens, O. G., *Applied Hydro- and Aero-Mechanics*, Dover Publications, Inc., New York, N.Y., 1957, 311 pp.
- Sirmans, Dale, Watts, Walter L., and Horwedel, Jon H., "Weather Radar Signal Processing and Recording at the National Severe Storms Laboratory," *IEEE Transactions of Geoscience Electronics*, Vol. 8, No. 2, Institute of Electrical and Electronic Engineers, New York, N.Y., Apr. 1970, pp. 88-94.
- Stout, G. E., and Hiser, H. W., "Radarscope Interpretations of Wind, Hail, and Heavy Rain Storms Between May 27 and June 8, 1954," *Bulletin of the American Meteorological Society*, Vol. 36, No. 10, Dec. 1955, pp. 519-527.
- Wilk, Kenneth E., Watts, W. L., Sirmans, D., Lhermitte, R. M., Kessler, E., and Gray, K. C., "Radar Measurements of Precipitation for Hydrological Purposes," *World Meteorological Organization International Hydrological Decade (IHD) Reports on WMO/IHD Projects Report No. 5*, Geneva, Switzerland, 1968, pp. 30-46.
- Zimmerman Leon I., "Atmospheric Wake Phenomena Near the Canary Islands," *Journal of Applied Meteorology*, Vol. 8, No. 6, Dec. 1969, pp. 896-907.

[Received September 23, 1971; revised March 15, 1972]